Journal of Molecular Structure 964 (2010) 109–118

Contents lists available at ScienceDirect

Journal of Molecular Structure

journal homepage: www.elsevier.com/locate/molstruc

Syntheses and structural characterization of three coordination polymers of Cd(II), Zn(II) and Pb(II) with the “V” shape ligand 4,4′-[isopropylidenebis(*p*-phenyleneoxy)]diacetic acid

Ze-Bao Zheng [a,]*, Ren-Tao Wu [a], Ji-Kun Li [b], Yi-Feng Sun [a], Yin-Feng Han [a]

[a] *Department of Chemistry and Environmental Science, Taishan University, Taian, Shandong 271021, PR China*
[b] *Department of Materials and Chemical Engineering, Taishan University, Taian, Shandong 271021, PR China*

ARTICLE INFO

Article history:
Received 6 September 2009
Accepted 5 November 2009
Available online 11 November 2009

Keywords:
4,4′-[Isopropylidenebis-(*p*-phenyleneoxy)]diacetic acid
“V” shape building block
Coordination polymers
Heterometallic

ABSTRACT

Three new inorganic–organic coordination polymers based on a “V” shape linking unit 4,4′-[isopropylidenebis(*p*-phenyleneoxy)]diacetic acid ($H_2\mathbf{L}$) and Cd^{II}, Zn^{II} and Pb^{II} ions, $[Cd(\mathbf{L})(H_2O)_2]_n$ (**1**), $[Zn_2(\mathbf{L})_3(H_2O)_6 \cdot 6H_2O]_n$ (**2**) and $[Pb_2Na_2(L)_3(DMF)_4(H_2O)_2 \cdot 2H_2O]_n$ (**3**), have been prepared and structurally characterized by single-crystal X-ray diffraction analysis. Complex **1** is a 1D zig-zag chain coordination polymer, which is connected by strong hydrogen-bond interactions to result in a 3D network. In complex **2**, an infinite 2D (6, 3) network with large hexagonal cavities was created. The whole 2D structure is a noninterpenetrating framework stacked by hydrogen-bonding interactions. Complex **3** is a novel 3D heterometallic coordination polymer, which possesses three different types of isolated channels.

1. Introduction

Nowadays, the design and preparation of metal–organic frameworks (MOFs) are still one of the most focused areas of research [1–4]. The rational design and synthesis of such novel coordination polymers are of great current interest in the field of supramolecular chemistry and crystal engineering [5–7], not only because of their intriguing structural motifs, but also because of their potential for a variety of applications [8–10]. As far as we know, the formation of MOFs is influenced by many factors, such as metal ions, organic ligands, counterions, solvent molecules and pH of the reaction mixture, etc. [11,12]. Among these factors, the selection of organic ligands is one of the most important aspects [13,14]. The configuration, rigidity, substituent and coordination modes of organic ligands have an important effect on the final structures. One of the most efficient routes to coordination polymers is to employ a multifunctional ligand to link metal ions into an infinite framework. Flexible di- and polycarboxylic acids are good candidates for the construction of novel metal–organic compounds as the carboxyl groups can form C—O—M—O four-membered rings with central metal ions, thereby improving the stability of transition metal–organic frameworks (MOFs). Furthermore, di- and polycarboxylic acids have two or more carboxyl groups that can be completely or partially deprotonated, which results in a rich variety of coordination modes and many interesting structures with higher dimensions. In light of the above, more and more attention has been paid to the use of flexible di- and polycarboxylate ligands [15–17], whereas studies involving semi-rigid V-shaped dicarboxylate ligands are relatively scarce [18–22]. 4,4′-[Isopropylidenebis(*p*-phenyleneoxy)]diacetic acid is a typical example of semi-rigid V-shaped dicarboxylate ligands. To the best of our knowledge, there has been no report about its coordination compounds. Herein, we report the synthesis and structures of three novel coordination polymers of 4,4′-[isopropylidenebis(*p*-phenyleneoxy)]diacetic acid, namely $[Cd(\mathbf{L})(H_2O)_2]_n$ (**1**), $[Zn_2(\mathbf{L})_3(H_2O)_6 \cdot 6H_2O]_n$ (**2**) and $[Pb_2Na_2(L)_3(DMF)_4(H_2O)_2 \cdot 2H_2O]_n$ (**3**).

2. Experimental

2.1. Materials and methods

The solvents and reagents for synthesis were commercially available and used as received. The ligand 4,4′-[isopropylidenebis(*p*-phenyleneoxy)]diacetic acid ($H_2\mathbf{L}$) was synthesized by the literature method [23]. Elemental analyses (C, H and N) were performed on a Perkin-Elmer 240C analyzer and IR spectra were measured on a Tensor 27 OPUS (Bruker) FT-IR spectrometer with KBr pellets. Thermogravimetric analysis (TGA) were carried out on a Delta Series TA-SDTQ600 in nitrogen atmosphere from room

---

* Corresponding author. Address: Department of Chemistry and Environmental Science, Taishan University, Yingbin Street, Taian, Shandong 271021, PR China. Tel.: +86 538 6715546; fax: +86 538 6715546.
E-mail address: zhengzebao@163.com (Z.-B. Zheng).

0022-2860/$ - see front matter © 2009 Elsevier B.V. All rights reserved.
doi:10.1016/j.molstruc.2009.11.018

Table 1
Crystal, data collection and structure refinement parameters for complexes **1–3.**

Complex	**1**	**2**	**3**
Empirical formula	$C_{19}H_{22}CdO_8$	$C_{57}H_{78}Zn_2O_{30}$	$C_{69}H_{90}Pb_2Na_2N_4O_{26}$
Formula weight	490.77	1373.93	1851.81
Wavelength, (Å)	0.71073	0.71073	0.71073
Crystal system	Orthorhombic	Trigonal	Monoclinic
Space group	*Ama2*	*P-3c1*	*C2/c*
a (Å)	28.130(6)	20.411(8)	39.364(3)
b (Å)	11.847(2)	20.411(8)	22.001(2)
c (Å)	5.588(1)	9.784(7)	8.846(7)
α (°)	90	90	90
β (°)	90	90	96.888(3)
γ (°)	90	120	90
Z	4	2	4
D_{calc}(Mg m^{-3})	1.750	1.293	1.617
F(000)	992	1440	3704
μ (mm^{-1})	1.218	0.759	4.513
Crystal size (mm)	0.28 × 0.20 × 0.15	0.15 × 0.13 × 0.11	0.30 × 0.18 × 0.08
θ Range (°)	2.90–24.97	2.00–25.05	1.04–25.00
Index ranges	$-33 \leqslant h \leqslant 32$; $-14 \leqslant k \leqslant 13$; $-6 \leqslant l \leqslant 6$	$-23 \leqslant h \leqslant 24$; $-19 \leqslant k \leqslant 24$; $-11 \leqslant l \leqslant 11$	$-46 \leqslant h \leqslant 46$; $-26 \leqslant k \leqslant 26$; $-9 \leqslant l \leqslant 10$
Reflections collected	10,128	17,528	43,026
Unique reflections	1660 (R_{int} = 0.0557)	2040 (R_{int} = 0.0883)	6717 (R_{int} = 0.0677)
Data/restraints/parameters	1660/0/135	2040/0/136	6717/0/494
Goodness of fit on F^2	1.194	1.009	1.113
Final R indices [$I > 2\sigma(I)$]	$R1$ = 0.0706, $wR2$ = 0.1597	$R1$ = 0.0699, $wR2$ = 0.1858	$R1$ = 0.0371, $wR2$ = 0.0969
R indices(all data)	$R1$ = 0.0740, $wR2$ = 0.1614	R1 = 0.1194, $wR2$ = 0.2255	$R1$ = 0.0529, $wR2$ = 0.1118
Largest difference in peak and hole (e Å^{-3})	2.309/−0.917	0.616/−0.420	1.238/−1.197

Table 2
Selected bond lengths (Å) and angles (°) for complexes **1–3**.

Compound **1**			
Cd(1)—O(4)	2.212(7)	Cd(1)—O(2)	2.351(8)
Cd(1)—O(3)	2.444(7)		
O(4)—Cd(1)—O(4)#1	95.9(5)	O(2)#1—Cd(1)—O(3)	87.5(3)
O(4)—Cd(1)—O(2)#1	141.9(3)	O(2)—Cd(1)—O(3)	55.0(2)
O(4)—Cd(1)—O(2)	102.6(3)	O(4)#1—Cd(1)—O(3)#1	126.6(3)
O(2)#1—Cd(1)—O(2)	82.6(4)	O(4)#1—Cd(1)—O(3)	87.3(3)
O(4)—Cd(1)—O(3)	126.6(3)	O(3)—Cd(1)—O(3)#1	131.5(3)
Compound **2**			
Zn(1)—O(2)	2.117(4)	Zn(1)—O(4)	2.120(4)
O(2)—Zn(1)—O(2)#2	88.90(13)	O(4)—Zn(1)—O(4) #2	88.37(14)
O(2)—Zn(1)—O(4)	89.61(14)	O(2)—Zn(1)—O(4) #2	93.17(14)
O(2)#2—Zn(1)—O(4)	177.42(14)		
Compound **3**			
Pb(1)—O(10)	2.431(4)	Pb(1)—O(9)	3.158(2)
Pb(1)—O(3)	2.439(4)	Na(1)—O(1)	2.369(4)
Pb(1)—O(2)	2.444(4)	Na(1)—O(11)	2.374(5)
Pb(1)—O(4)	2.762(4)	Na(1)—O(12)	2.416(5)
Pb(1)—O(1)	2.835(3)	Na(1)—O(2)#3	2.434(4)
Pb(1)—O(8)	2.850(4)	Na(1)—O(3)#3	2.469(5)
Pb(1)—O(10) #3	2.891(4)	Na(1)—O9	2.479(4)
Pb(1)—O(3) #3	3.075(2)		
O(10)—Pb(1)—O(3)	78.86(14)	O(12)—Na(1)—O(2)#3	99.42(18)
O(10)—Pb(1)—O(2)	84.56(13)	O(1)—Na(1)—O(3)#3	101.24(15)
O(3)—Pb(1)—O(2)	70.02(13)	O(11)—Na(1)—O(3)#3	97.34(18)
O(10)—Pb(1)—O(4)	116.11(13)	O(12)—Na(1)—O(3)#3	168.34(18)
O(3)—Pb(1)—O(4)	49.69(13)	O(2)#3—Na(1)—O(3)#3	69.68(13)
O(2)—Pb(1)—O(4)	105.39(13)	O(1)—Na(1)—O9	82.08(14)
O(1)—Na(1)—O(11)	161.33(19)	O(11)—Na(1)—O9	98.67(17)
O(1)—Na(1)—O(12)	73.41(15)	O(12)—Na(1)—O9	106.79(19)
O(11)—Na(1)—O(12)	88.65(18)	O(2)#3—Na(1)—O9	147.41(15)
O(1)—Na(1)—O(2)#3	87.31(15)	O(3)#3—Na(1)—O9	82.27(15)
O(11)—Na(1)—O(2)#3	101.01(17)		

Symmetry transformations used to generate equivalent atoms: #1 $-x+1, -y, z$; #2 $-y+1, x-y, z$; #3 $x, -y+1, z-½$.

temperature to 1000 °C (heating rate = 10 °C min^{-1}) using aluminium crucibles.

2.2. Syntheses

2.2.1. [Cd(**L**)(H_2O)$_2$]$_n$ (**1**)

A mixture of $Cd(CH_3COO)_2 \cdot 2H_2O$ (0.135 g, 0.5 mmol) and H_2**L** (0.172 g, 0.5 mmol) were dissolved in water (12 ml) and ethanol (3 ml), the pH of the solution was adjusted to be about 6–7 with 0.2 mol L^{-1} aqueous NaOH, then the mixed solution was stirred for 30 min at room temperature, transferred to and sealed in a 25 ml Teflon-lined stainless steel reactor, and then heated at 140 °C for 72 h, upon cooling to room temperature, colorless acicular single crystals were collected and dried in air. Yield: 40% (based on Cd). Anal. Calcd. for $C_{19}H_{22}CdO_8$: C, 46.50; H, 4.52. Found: C, 46.39; H, 4.43. IR (KBr, cm^{-1}): 3410(s), 2928(w), 2849(w), 1607(m), 1563(s), 1512(s), 1434(m), 1339(s), 1248(s), 1188(m), 1073(m), 835(m), 737(w), 570(w).

2.2.2. [Zn_2(**L**)$_3$(H_2O)$_6$·6H_2O]$_n$ (**2**)

A buffer layer of CH_3OH/DMF (6 ml, 1:1) was carefully layered over a water (4 ml) solution of $Zn(OAc)_2$ (22 mg, 0.1 mmol). Then a solution of H_2**L** (35 mg, 0.1 mmol) in methanol (3 ml) was layered

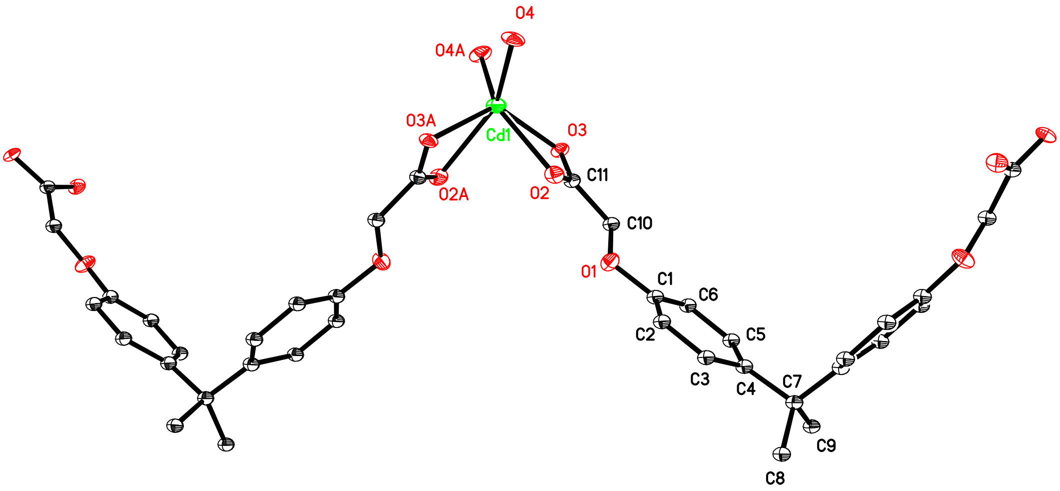

Fig. 1. View of the metal coordination environment in **1** (H atoms are omitted for clarity).

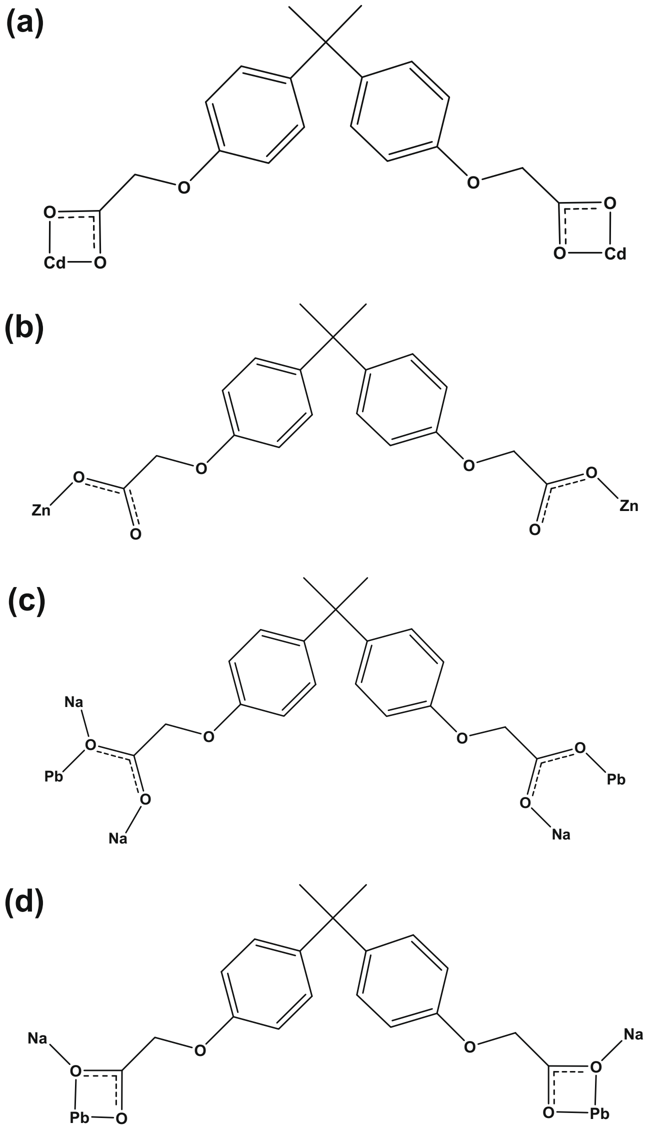

Scheme 1. The coordination mode of **L**.

on the buffer layer in a test tube. After 20 days, colorless block single crystal appeared at the buffer layer were collected. Yield (based on Zn): 30%. Anal. Calcd. for $C_{57}H_{78}Zn_2O_{30}$: C, 49.83; H, 5.72; Found: C, 49.75; H, 5.81. IR (cm^{-1}): 3411(s), 2915(w), 2832(w), 1639(s), 1526(m), 1445(s), 1337(m), 1255(m), 1086(m), 845(w), 773(s), 497(m).

2.2.3. $[Pb_2Na_2(L)_3(DMF)_4(H_2O)_2\cdot 2H_2O]_n$ (**3**)

A mixture of $Pb(CH_3COO)_2\cdot 3H_2O$ (0.379 g, 1 mmol), H_2**L** (0.344 g, 1 mmol) and NaOH (0.080 g, 2 mmol) were dissolved in DMF (12 ml) and water (3 ml), the mixed solution was stirred at 60 °C for 3 h. Upon cooling to room temperature, the solution was filtered and the filtrate was allowed to stand at room temperature. After slow evaporation over 2 weeks, colorless acicular single crystals were obtained. Yield: 60% based on Pb. Anal. Calcd. for $C_{69}H_{90}Na_2Pb_2N_4O_{26}$: C, 44.75; H, 4.90; N, 3.02. Found: C, 43.93; H, 4.58; N, 3.42. IR (KBr, cm^{-1}): 3470(s), 2959(w), 2871(w), 1657(m), 1608(s), 1506(m), 1421(m), 1322(m), 1244(s), 1188(m), 1058(m), 832(s), 721(w), 532(w).

2.3. X-ray crystallography

X-ray single-crystal diffraction data for complexes **1**–**3** were collected on a Bruker APEX-II area-detector diffractometer with Mo Kα radiation ($\lambda = 0.71073$ Å). Absorption corrections were applied by SADABS. All the structures were solved by direct methods using the SHELXS program of the SHELXTL package and refined by full-matrix least-squares methods with SHELXL [24]. Metal atoms in each complex were located from the *E*-maps and other non-hydrogen atoms were located in successive difference Fourier syntheses and refined with anisotropic thermal parameters on F^2. The hydrogen atoms of the ligand were generated theoretically onto the specific atoms and refined isotropically with fixed thermal factors. The disordered groups of DMF molecules in **3** were split in two positions in the refinement.

Crystallographic data and experimental details for structural analyses are summarized in Table 1. Selected bond lengths and angles are listed in Table 2.

3. Results and discussion

3.1. Description of crystal structures

3.1.1. $[Cd(\mathbf{L})(H_2O)_2]_n$ (**1**)

As illustrated in Fig. 1, each Cd(II) atom in **1** is coordinated by six oxygen atoms from two chelating carboxylate groups of two **L** ligands and two water molecules. The coordination sphere of the Cd(II) center is best described as a trapezoidal bipyramid. The O2, O3, O3A, O4A atoms define the equatorial plane. The axial positions are occupied by O2A and O4 atoms with O2A—Cd—O4

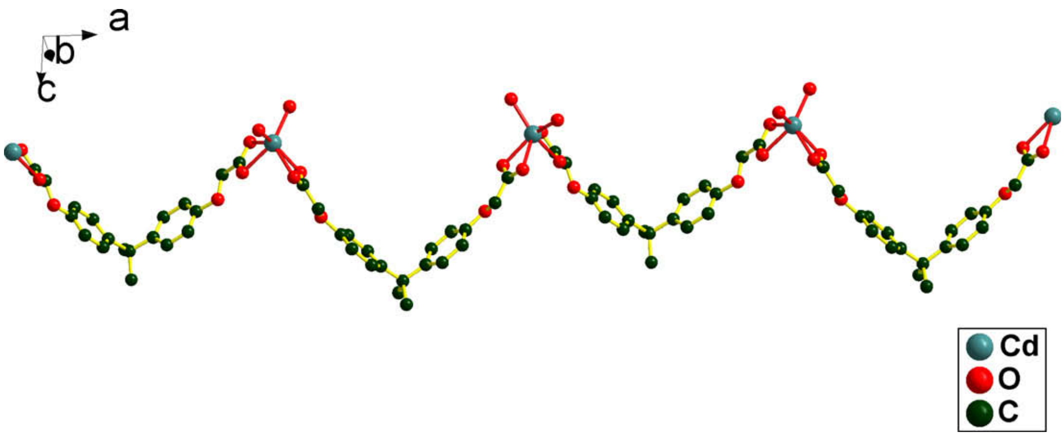

Fig. 2. The 1D zig-zag chain structure of **1** viewed along the *a*-axis.

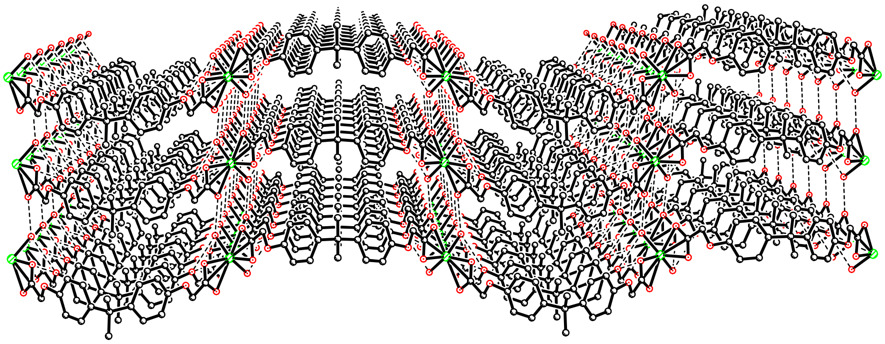

Fig. 3. Perspective view of the 3D supramolecular networks of complex **1**.

angle of 141.9(3)°. Which is similar to the Cd(II) complex of phenoxyacetic acid [25].

Each **L** ligand bridges two cadmium atoms in a chelating/chelating bis(bidentate) coordination mode (Scheme 1a) to form a 1D infinite zig-zag chain (Fig. 2) along the *a*-axis with a Cd···Cd distance of 14.065(3) Å. Interestingly, these chains are interlinked by O—H···O hydrogen bonds produced by the **L** and coordinated water molecules[O4···O1A = 2.905 Å, O4···O2A = 2.762 Å and O4···O3B = 2.623 Å, and the angles O4—H12···O1A = 164.99°, O4—H12···O2A = 120.11°, O4—H11···O3B = 110.18° symmetry code A: *x, y, z*−1; B: *x, y*−*1/2, z*−1/2] into a 3D network (Fig. 3).

3.1.2. $[\mathrm{Zn}_2(\mathbf{L})_3(\mathrm{H_2O})_6\cdot 6\mathrm{H_2O}]_n$ (**2**)

As shown in Fig. 4, each Zn center located on the crystallographic 3-fold axis is coordinated by three water molecules and three oxygen atoms of three distinct **L** ligands. The coordination polyhedron of the Zn(II) atom can be viewed as distorted octahedron. Each **L** ligand bridges two metal ions through two terminal carboxylate groups in monodentate coordination mode (Scheme 1b). The Zn centers serve as 3-connected nodes in the framework, thereby creating an infinite two-dimensional (6, 3) network, which contains large edge-sharing hexagons with a metal ion at each corner and **L** ligand molecule at each edge (Fig. 5). The hexagonal grids

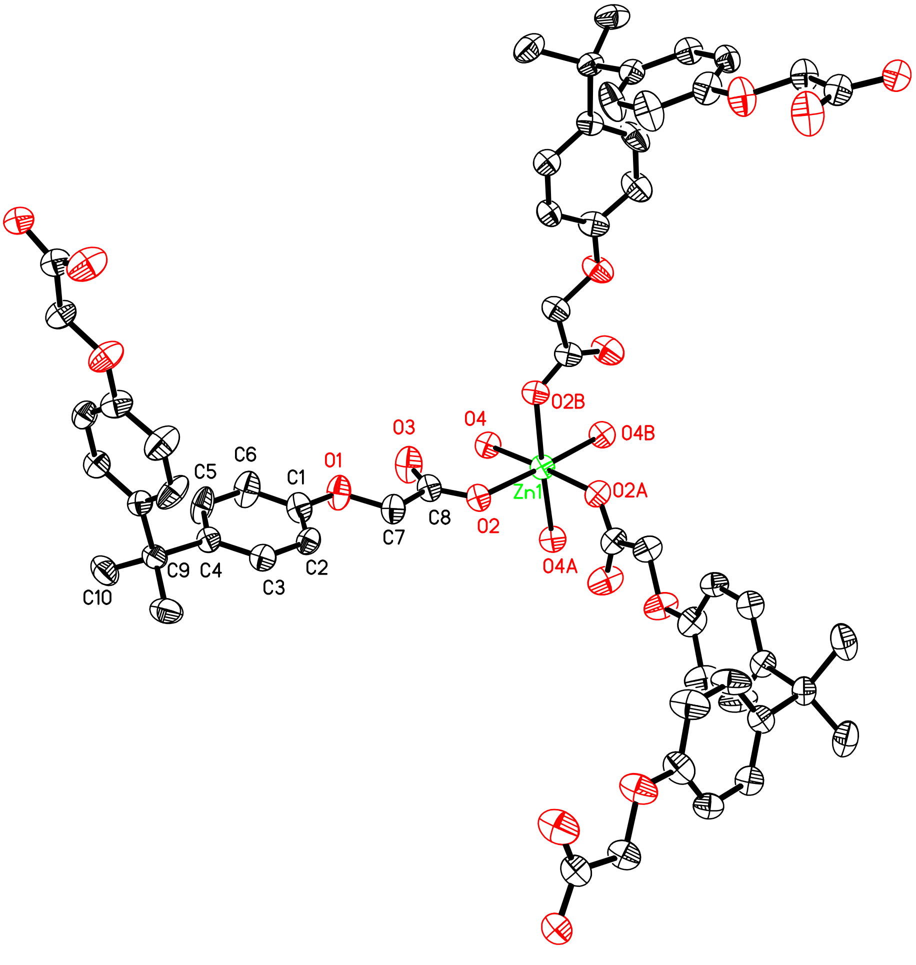

Fig. 4. View of the metal coordination environment in **2** (H atoms and lattice water are omitted for clarity).

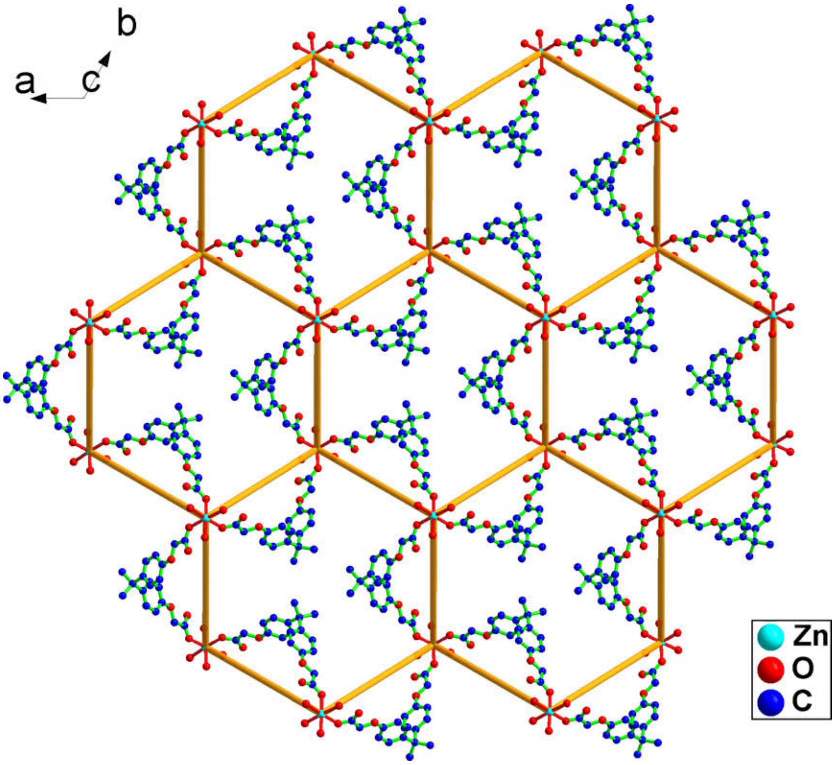

Fig. 5. Perspective view of the 2D (6, 3) layer of complex **2**, the H atoms and lattice water are omitted for clarity.

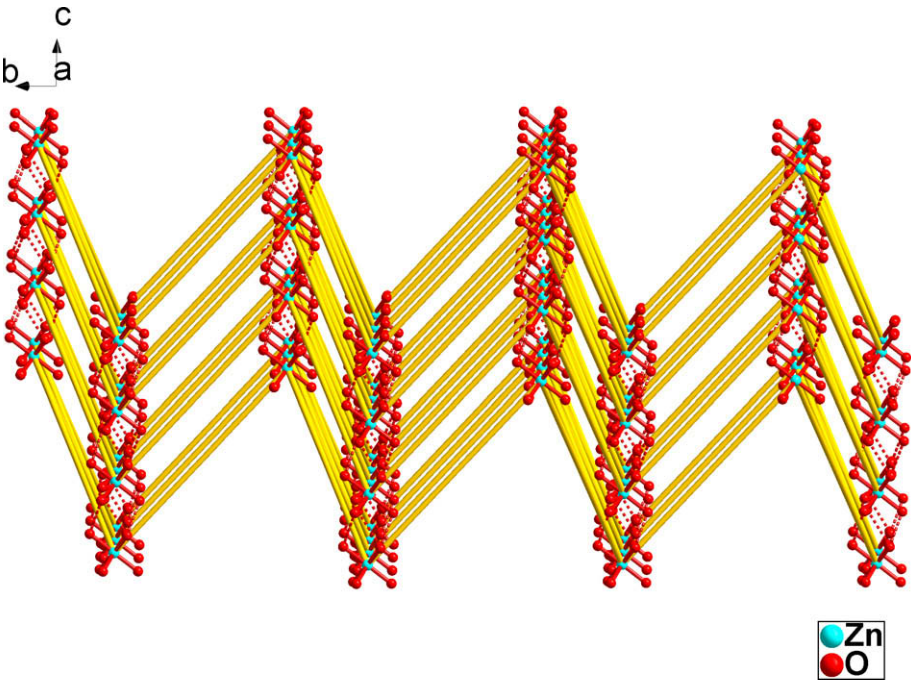

Fig. 6. Schematic representation of **2**, showing the stacking of the noninterpenetrating (6, 3) networks. The lines represent ligand molecules.

exhibit identical edge lengths [17.56(1) Å] and identical corner angles [71.06(1)°], and the separation of the opposite corner is 26.92(6) Å. Because of the length and flexibility of the **L** ligand, the metal ions of (6, 3) network do not lie in the same plane but represent a chair conformation.

It should be pointed out that, the 2D coordination networks of **2** do not interpenetrate each other, which is rare in such large macrometallacycle frameworks [26,27]. In addition, in the crystal structure such 2D layers are interlinked by O—H···O hydrogen bonds [O4···O2A = 2.856 Å and the angles O4—H12···O2A =

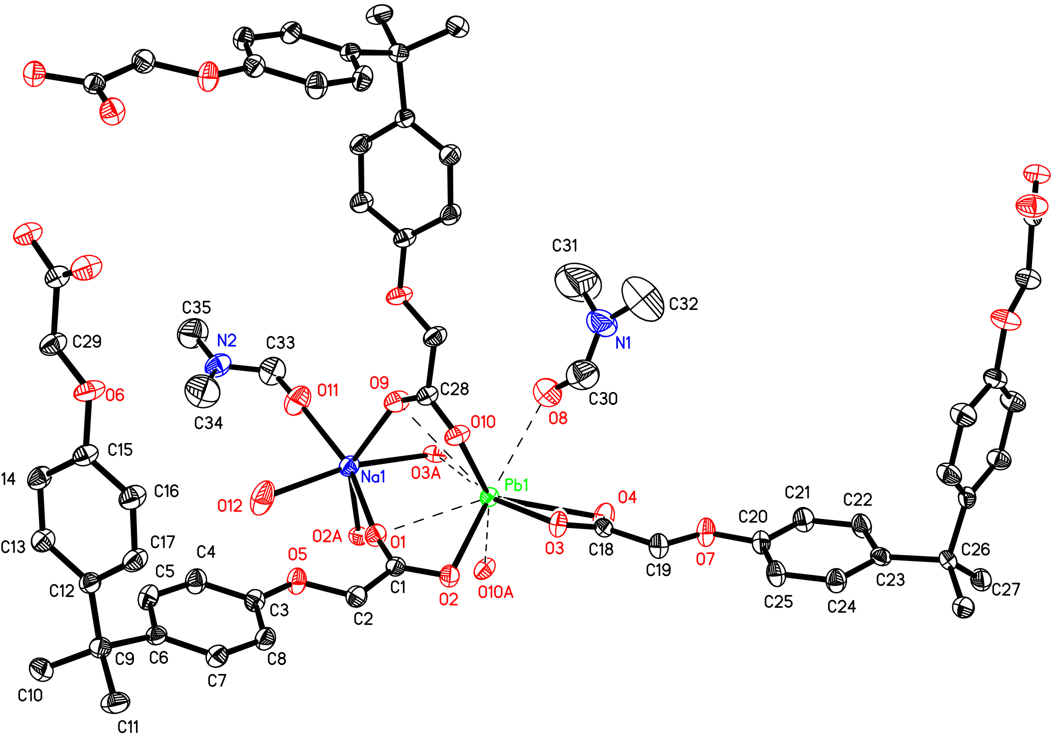

Fig. 7. Molecular structure of complex **3** with 30% probability ellipsoids. Hydrogen atoms are omitted for clarity.

132.93°, symmetry code A: $-y+1$, $-x+1$, $z-1/2$] to finish the 3D stacking (Fig. 6).

3.1.3. [$Pb_2Na_2(L)_3(DMF)_4(H_2O)_2 \cdot 2H_2O]_n$ (**3**)

As shown in Fig. 7, the sodium ion was located in a distorted octahedral coordination environment. The axis position was occupied by a DMF and a carboxylate oxygen atom of **L**, respectively. Three oxygen atoms from carboxyl groups of **L** and a water molecule are in the equatorial positions. The Pb(II) ion is four-coordinate with four carboxylate oxygen atoms from three different **L** ligands and exhibits a tetrahedral geometry. The four oxygen atoms are located on one side of the Pb(II) ion which adopts a hemidirected structural categories and shows the presence of a stereochemically active lone electron pair [28,29]. Indeed, when the bonding limit of Pb—O in complex **3** extends from 2.76 to 3.16 Å, the potential weak reactions (represented as dashed in Fig. 7) are found. The five weak bonds in the direction of the void complete the coordination sphere and increase the coordination number of Pb(II) from four to nine. For all of the nine bonds around Pb(II) are comparatively symmetrical, the coordination geometry of Pb(II) in **3** can be viewed as holodirected [30,31].

In complex **3**, the **L** ligands show two different coordination modes. One is a pentadentate chelating and bridging coordination mode (Scheme 1c), on the basis of this connection mode, the heterometallic ions Na(I) and Pb(II) were bridged by **L** ligands to form a 2D layer of composition $[Na_2Pb_2(L)_2]_n$ (Figs. 8a), which constructed by square shaped tubular channels (channel A with dimensions of approximately 10 × 10 Å) edge-sharing the 1D metal/carboxylate chains (Figs. 8b). The layers are further linked by other **L** ligands in a chelating-bridging tridentate/chelating-bridging tridentate coordination mode (Scheme 1d) to generate a novel 3D channeled framework (Fig. 9). Which still have two other parallel tunnels except the square shaped channels mentioned above: one square shaped (channel B with dimensions of approximately 10 × 10 Å) and one hexagonal (channel C with interatomic distances approximately 9 Å) (Fig. 9a). The square shaped channels filled by the guest DMF and water molecules, and the hexagonal channels are empty (Fig. 9b). The van der Waals free space of the voids per unit cell (after the solvent water molecules have been hypothetically removed) is approximately 2810 Å^3, corresponding to 37.0% of the volume of the unit cell (calculated by Platon) [32].

From the topological point of view, the 3D structure of **3** can be simplified to a unique (3, 4, 4, 5)-connected net with an unprecedented $\{4^2;6\}_2\{4^2;8^3;10\}\{4^2;8^4\}_2\{4^7;6^3\}_2$ topology (Fig. 10) [33,34]. In this simplification, the Pb(II) atom acts as the three-connected node $\{4^2;6\}_2$, the Na(I) atom acts as one kind of the four-connected node $\{4^2;8^3;10\}$, the **L** ligands with a chelating-bridging tridentate/chelating-bridging tridentate coordination mode as the other four-connected node$\{4^2;8^4\}_2$, and the other **L** ligands as five-connected node$\{4^7;6^3\}_2$.

3.2. Thermogravimetric analysis

Thermogravimetric analysis (TGA) for compounds **1**–**3** was performed under a flow of N_2 gas (Fig. 11). For compound **1**, its TG curve (Fig. 11a) shows three main steps of weight losses. The first step started at 100 and completed at 130 °C, which corresponds to the release of two coordination water molecules. The observed weight-loss of 7.80% is close to the calculated value (7.34%). The second and third steps (310–560 °C) corresponds to the release of **L** ligands, giving cadmium oxides as the final decomposition product which constitutes 26.54% (calcd. 26.17%). TG curve (Fig. 11b) of **2** exhibits three steps of weight losses. The weight-loss of 15.26% during the first and two steps from 50 to 150 °C corresponds to the loss of six crystal-lattice water molecules and six coordination water molecules (calcd. 15.74%). The third step (330–550 °C) corresponds to the release of L ligands, giving ZnO as the final decomposition product which constitute 12.46% (calcd. 11.85%).

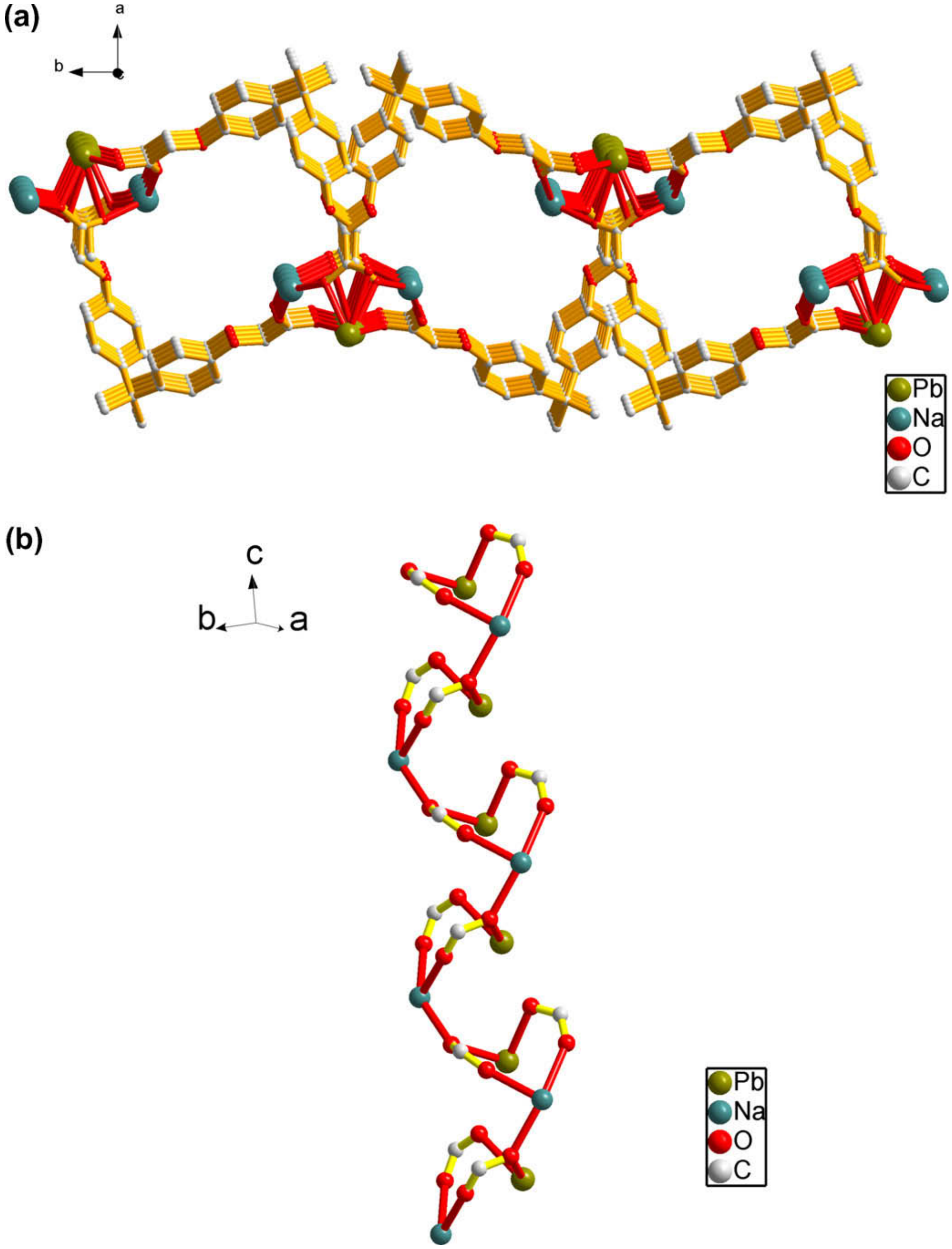

Fig. 8. (a) Perspective view of the 2D supramolecular layer of composition $[Na_2Pb_2(L)_2]_n$. (b) Propagation in the *c*-direction of the chain, built up by the metals bridged by carboxyl groups of **L**.

As shown in Fig. 11c, compound **3** loses all DMF and water molecules in the range 50–301 °C with a weight-loss of 19.11% (calcd. 19.68%). One **L** ligand is released in 347–434 °C with a weight-loss of 19.25% (calcd. 18.47%), resulting in an intermediate product $[Na_2Pb_2(L)_2]$ formed. This intermediate specie is further decomposed in 700–900 °C with a final residue $Na_2Pb_2O_3$ formed (found 15.85%, calcd. 16.26%).

4. Conclusions

Three coordination polymers of a "V" shape ligand 4,4′-[isopropylidenebis(*p*-phenyleneoxy)diacetic acid (H_2**L**) with the Cd(II), Zn(II) and Pb(II) ions have been synthesized under room solution or hydrothermal reactions, and structurally characterized by X-ray diffraction analysis. These compounds show 1D, 2D and 3D coordination frameworks, respectively. The present study demonstrates that the "V" shape **L** anion is capable of coordination to metal centers in variable coordination modes, and the MOFs exhibit different dimensionalities with different metal ions, as well as that the coordination geometry of the metal ions is very important for the formation of acentric crystal structures. Meanwhile, the intramolecular/intermolecular hydrogen-bonding interaction, play an important role in the formation of complexes, especially linking the discrete subunits or low-dimensional entities into high dimensional frameworks.

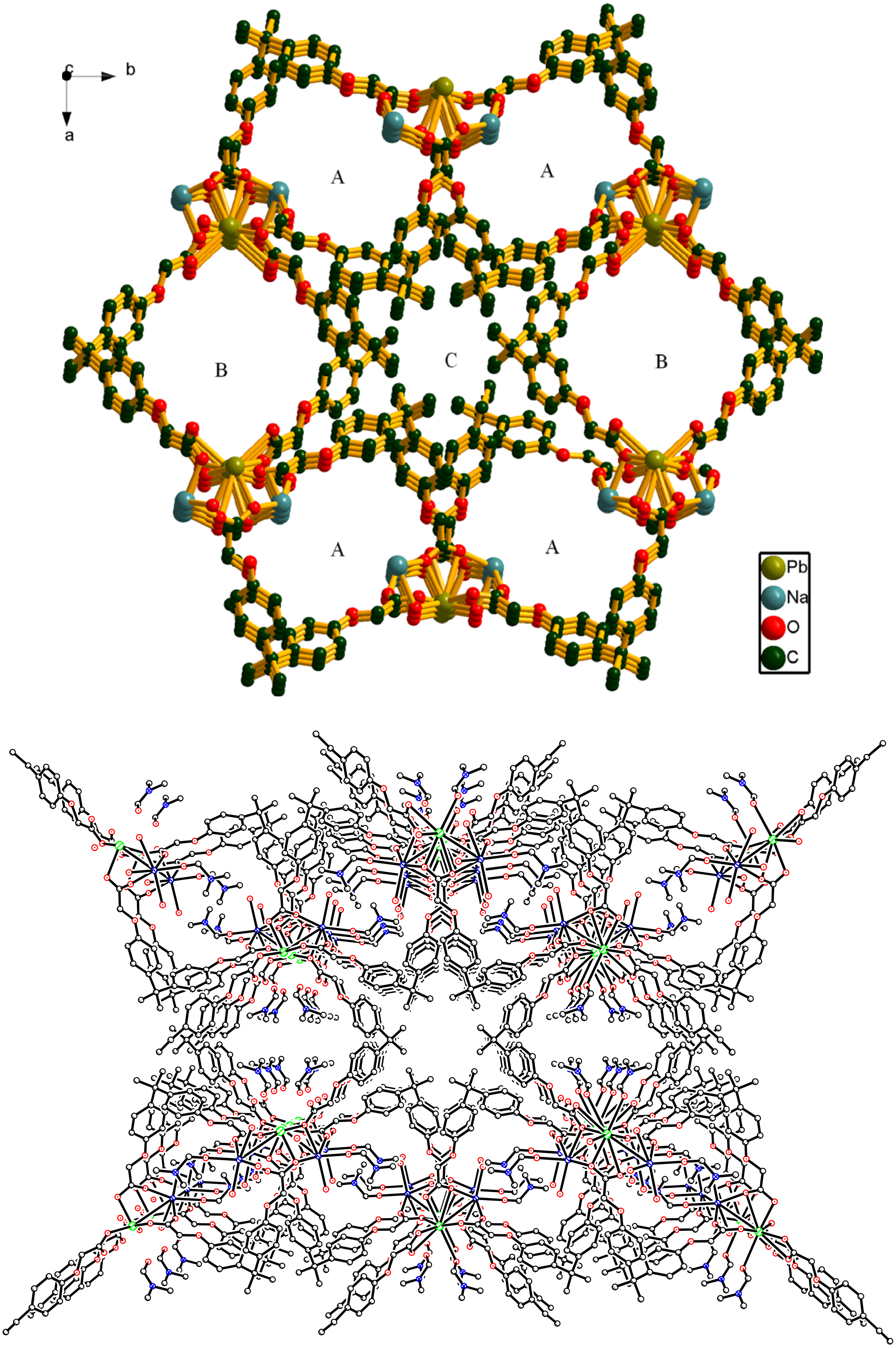

Fig. 9. (a) View of the packing diagram along the *c*-direction, with the different channels presented, hydrogen atoms and solvent molecules are omitted for sake of clarity. (b) View of the square column filled by the guest DMF and water molecules.

Supplementary material

Crystallographic data (excluding structure factors) for the structure analyses of complexes **1**–**3** have been deposited with the Cambridge Crystallographic Data Center, CCDC No. 658571 **1**, 744704 **2** and 658570 **3**. Copies of these information may be obtained free of charge on application to the Director, CCDC, 12 Union Road, Cambridge, CB2 1EZ, UK (Fax: +44 1223 336033; e-mail: deposit@ccdc.cam.ac.uk or http://www.ccdc.cam.ac.uk).

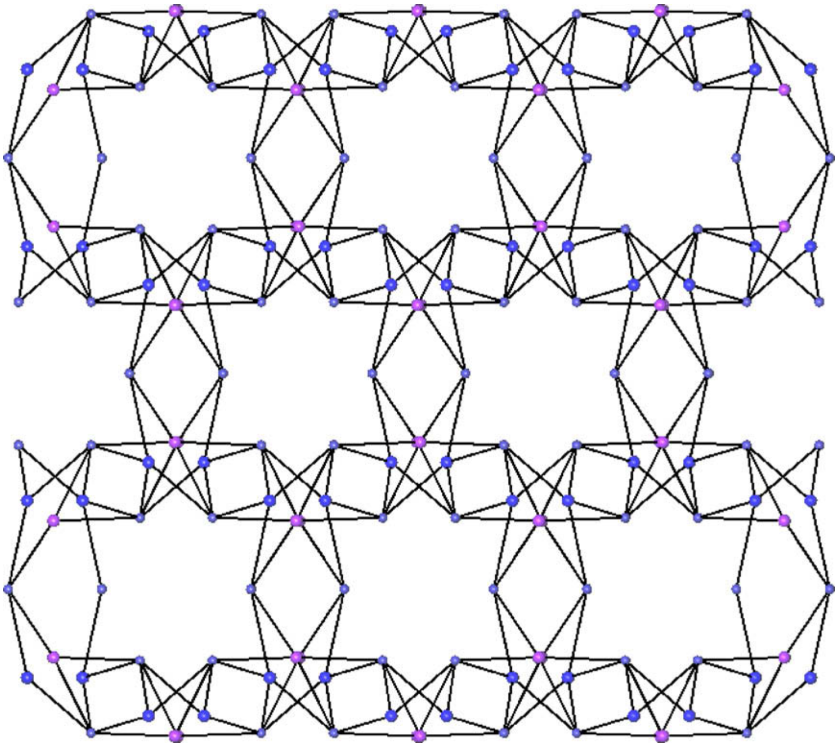

Fig. 10. Schematic illustration of the (3, 4, 4, 5)-connected 3D net. Color scheme: Pb, pink; Na, dark blue; L, pale blue. (For interpretation of the references to color in this figure legend, the reader is referred to the web version of this paper.)

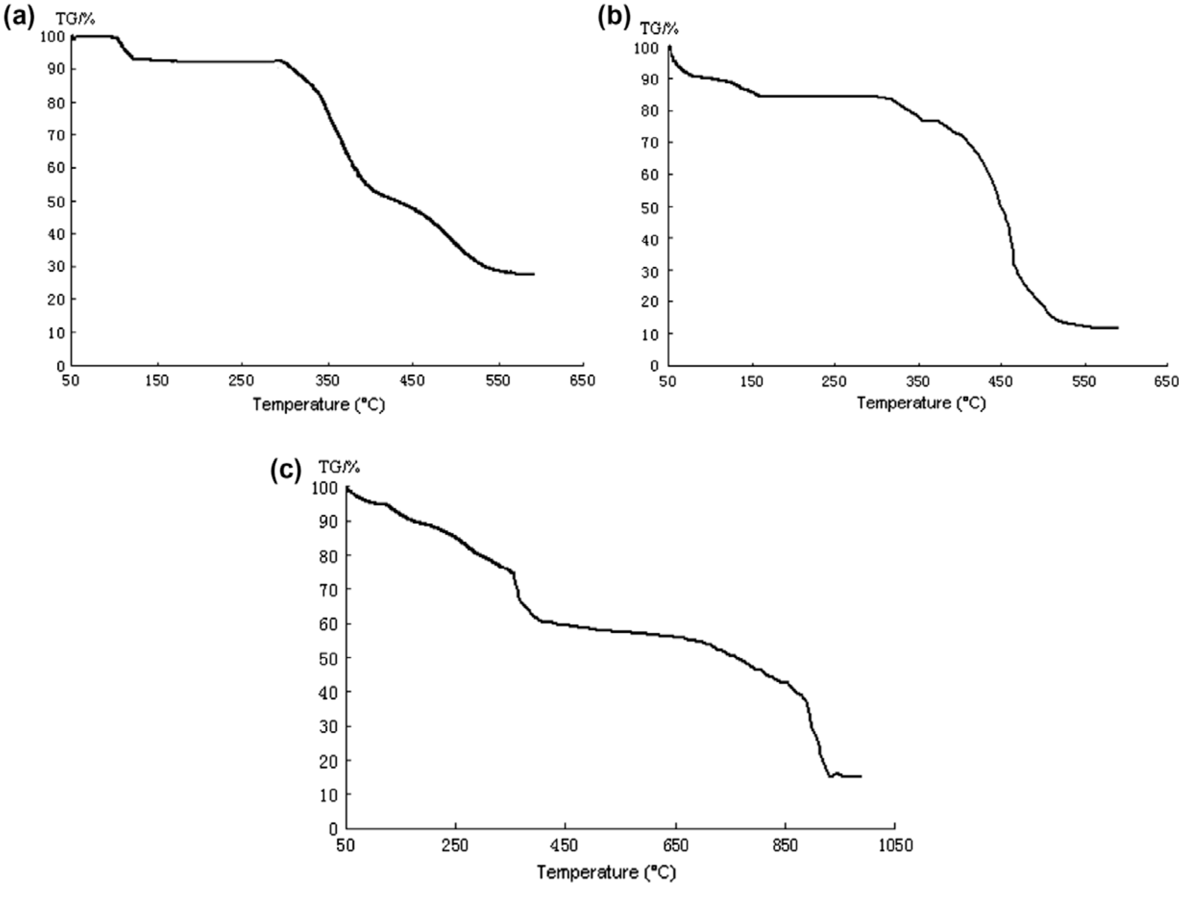

Fig. 11. TG curves of compounds **1**–**3**.

Acknowledgements

We acknowledge the Postgraduate Foundation of Taishan University (No.Y05-2-02).

References

[1] N.L. Rosi, J. Eckert, M. Eddaoudi, D.T. Vodak, J. Kim, M. O'Keeffe, O.M. Yaghi, Science 300 (2003) 1127.
[2] S.J. Dalgarno, N.P. Power, J.L. Atwood, Coord. Chem. Rev. 252 (2008) 825.
[3] J.G. Vitillo, L. Regli, S. Chavan, G. Ricchiardi, G. Spoto, P.D.C. Dietzel, S. Bordiga, A. Zecchina, J. Am. Chem. Soc. 130 (2008) 8386.
[4] C.Y. Sun, S.X. Liu, D.D. Liang, K.Z. Shao, Y.H. Ren, Z.M. Su, J. Am. Chem. Soc. 131 (2009) 1883.
[5] J.W. Steed, J.L. Atwood, Supramolecular Chemistry, Wiley and Sons, New York, 2000.
[6] B. Moulton, M. Zworotko, Chem. Rev. 101 (2001) 1629.
[7] C.L. Chen, J.Y. Zhang, C.Y. Su, Eur. J. Inorg. Chem. (2007) 2997.
[8] H.K. Chae, D.Y. Siberio-Perez, J. Kim, Y.B. Go, M. Eddaoudi, A.J. Matzger, M. O'Keeffe, O.M. Yaghi, Nature 427 (2004) 523.
[9] D.M. Bassani, V. Darcos, S. Mahony, J.P. Desvergne, J. Am. Chem. Soc. 122 (2000) 8795.
[10] M.W. Hosseini, Acc. Chem. Res. 38 (2005) 313;.
[11] S.M. Chen, C.Z. Lu, Q.Z. Zhang, J.H. Liu, X.Y. Wu, Eur. J. Inorg. Chem. (2005) 423.
[12] P.M. Forster, N. Stock, A.K. Cheetham, Angew. Chem. Int. Ed. 44 (2005) 7608.
[13] A.J. Blake, N.R. Brooks, N.R. Champness, M. Crew, A. Deveson, D. Fenske, D.H. Gregory, L.R. Hanton, P. Hubberstey, M. Schröder, Chem. Commun. (2001) 1432.
[14] Y.J. Qi, Y.H. Wang, C.W. Hu, M.H. Cao, L. Mao, E.B. Wang, Inorg. Chem. 42 (2003) 8519.
[15] Z.H. Zhou, J.M. Yang, H.L. Wan, Cryst. Growth Des. 5 (2005) 1825.
[16] S.L. Childs, L.J. Chyall, J.T. Dunlap, V.N. Smolenskaya, B.C. Stahly, G.P. Stahly, J. Am. Chem. Soc. 126 (2004) 13335.
[17] D.T. de Lill, N.S. Gunning, C.L. Cahill, Inorg. Chem. 44 (2005) 258.
[18] D. Tanaka, K. Nakagawa, M. Higuchi, S. Horike, Y. Kubota, T.C. Kobayashi, M. Takata, S. Kitagawa, Angew. Chem. Int. Ed. 47 (2008) 3914.
[19] S.Q. Zang, Y. Su, Y.Z. Li, H.Z. Zhu, Q.J. Meng, Inorg. Chem. 45 (2006) 2972.
[20] P. Mahata, M. Prabu, S. Natarajan, Inorg. Chem. 47 (2008) 8451.
[21] X.L. Wang, C. Qin, E.B. Wang, Z.M. Su, Chem. Eur. J. 12 (2006) 2680.
[22] H. Furukawa, J. Kim, N.W. Ockwig, M. O'Keeffe, O.M. Yaghi, J. Am. Chem. Soc. 130 (2008) 11650.
[23] M. Inouye, T. Miyake, M. Furusyo, H. Nakazumi, J. Am. Chem. Soc. 117 (1995) 12416.
[24] G.M. Sheldrick, SHELXTL, Version 6.1, Bruker AXS Inc., Madison, WI, USA, 2000.
[25] T.C.W. Mak, W.H. Yip, E.J. O'Reilly, G. Smith, C.H.L. Kennard, Inorg. Chim. Acta 100 (1985) 267.
[26] K.T. Youm, S. Huh, Y.J. Park, S. Park, M.G. Chol, M.J. Jun, Chem. Commun. (2004) 2384.
[27] Y.Q. Sun, J. Zhang, Z.F. Ju, G.Y. Yang, Cryst. Growth Des. 5 (2005) 1939.
[28] P.P. Power, Chem. Rev. 99 (1999) 3463.
[29] Y.H. Zhao, H.B. Xu, Y.M. Fu, K.Z. Shao, S.Y. Yang, Z.M. Su, X.R. Hao, D.X. Zhu, E.B. Wang, Cryst. Growth Des. 8 (2008) 3566.
[30] D.J. Zhang, T.Y. Song, J. Shi, K.R. Ma, Y. Wang, L. Wang, P. Zhang, Y. Fan, J.N. Xu, Inorg. Chem. Commun. 11 (2008) 192.
[31] A. Morsali, A. Ramazanib, Z. Anorg. Allg. Chem. 631 (2005) 1759.
[32] P. Van der Sluis, A.L. Spek, Acta Crystallogr. A 46 (1990) 194.
[33] V.A. Blatov, A.P. Shevchenko, TOPOS-Version 4.0 Professional (Beta Evaluation), Samara State University, Samara, Russia, 2006.
[34] V.A. Blatov, A.P. Shevchenko, V.N. Serezhkin, J. Appl. Crystallogr. 33 (2000) 1193.